The Structure of Human Retinol-Binding Protein (RBP) with Its Carrier Protein Transthyretin Reveals an Interaction with the Carboxy Terminus of RBP[†,‡]

Helen M. Naylor and Marcia E. Newcomer*

Department of Biochemistry, Vanderbilt University School of Medicine, Nashville, Tennessee 37232-0146

Received September 23, 1998; Revised Manuscript Received December 17, 1998

ABSTRACT: Whether ultimately utilized as retinoic acid, retinal, or retinol, vitamin A is transported to the target cells as *all-trans*-retinol bound to retinol-binding protein (RBP). Circulating in the plasma, RBP itself is bound to transthyretin (TTR, previously referred to as thyroxine-binding prealbumin). In vitro one tetramer of TTR can bind two molecules of retinol-binding protein. However, the concentration of RBP in the plasma is limiting, and the complex isolated from serum is composed of TTR and RBP in a 1 to 1 stoichiometry. We report here the crystallographic structure at 3.2 Å of the protein−protein complex of human RBP and TTR. RBP binds at a 2-fold axis of symmetry in the TTR tetramer, and consequently the recognition site itself has 2-fold symmetry: Four TTR amino acids (Arg-21, Val-20, Leu-82, and Ile-84) are contributed by two monomers. Amino acids Trp-67, Phe-96, and Leu-63 and -97 from RBP are flanked by the symmetry-related side chains from TTR. In addition, the structure reveals an interaction of the carboxy terminus of RBP at the protein−protein recognition interface. This interaction, which involves Leu-182 and Leu-183 of RBP, is consistent with the observation that naturally occurring truncated forms of the protein are more readily cleared from plasma than full-length RBP. Complex formation prevents extensive loss of RBP through glomerular filtration, and the loss of Leu-182 and Leu-183 would result in a decreased affinity of RBP for TTR.

The transport of vitamin A to the target tissues is mediated by plasma retinol-binding protein (RBP).[1] This specific carrier protein for *all-trans*-retinol is synthesized primarily in the liver, where it requires the binding of retinol to trigger its secretion (*1*). Other sites of synthesis are known (*2*) and include the kidney, peritubular and Sertoli cells of the testis (*3*), and retinal pigment epithelium (*4*, *5*).

Whether ultimately utilized as retinoic acid, retinal, or retinol, vitamin A is transported to the target cells by RBP as *all-trans*-retinol, and only retinol triggers secretion of RBP (*1*). Circulating in the plasma, RBP is found bound to transthyretin (TTR, previously referred to as thyroxine-binding prealbumin). In vitro one tetramer of TTR can bind two molecules of retinol-binding protein. However, the concentration of RBP in the plasma is limiting, and the complex isolated from serum is composed of TTR and RBP in a 1 to 1 stoichiometry. Complex formation appears to be necessary to prevent extensive loss of the low molecular weight RBP through glomerular filtration (*6*) and may also restrict free partitioning of RBP into the intercellular space outside the vascular system. Furthermore, binding to TTR may be important for the secretion of newly synthesized holo-RBP (for review see ref *2*).

Well-refined X-ray structures are available for both transthyretin (*7*) and retinol-binding protein (*8*). Transthyretin is a homotetramer (55 kDa) which is best described as a dimer of dimers. Monomers associate via the formation of an eight-stranded antiparallel β-sheet to which each monomer contributes four β-strands. These β-sheets are back to back at the center of the tetramer, and there is a large solvent channel which passes between the two sheets in which two molecules of thyroxine can bind. A variety of naturally occurring mutations in transthyretin have been described, and the mutation of Ile-84 to Asn or Ser abrogates RBP−TTR complex formation. Individuals with this variant of TTR have substantially lowered plasma concentrations of RBP (*9*). Retinol-binding protein is a member of the lipocalin superfamily. It is composed of an eight-stranded β-barrel and a C-terminal α-helix and has a molecular mass of 21 kDa. The retinol is encapsulated by the β-barrel in the binding cavity in a hand-in-glove-like fit with the ring end of the retinol innermost. Only the hydroxyl of the retinol is solvent accessible (*8*). Apo-RBP has reduced affinity for transthyretin.

A structure of the mixed species complex of chicken RBP and human TTR has been described (*10*). Two molecules of RBP bind to the same TTR dimer at equivalent binding sites. Although the sequence of retinol-binding protein is highly conserved, chicken RBP lacks the carboxy-terminal eight amino acids characteristic of all mammalian RBP's, and a number of observations suggest that there is interaction of the carboxy terminus of RBP with TTR. In addition, chicken TTR can bind up to four molecules of chicken RBP (*11*). To determine whether there is an interaction of the carboxy

[†] This work was supported by an NIH grant (GM55420) to M.E.N. H.M.N. was supported by NIH Training Grant GM0820.

[‡] Coordinates have been deposited in the Protein Data Bank (filename 1qab).

* Corresponding author. Telephone: (615) 343-7333. Fax: (615) 343-1898. E-mail: newcomer@lhmrba.hh.vanderbilt.edu.

[1] Abbreviations: RBP, retinol-binding protein; TTR, transthyretin; FPLC, fast protein liquid chromatography.

10.1021/bi982291i CCC: $18.00
Published on Web 02/13/1999

terminus of human RBP with human TTR, we determined the crystal structure of the complex. In the human RBP−TTR complex, the C-terminus of RBP, which in the structure of RBP alone is disordered, is found nestled in a hydrophobic patch at the RBP−TTR interface.

MATERIALS AND METHODS

Protein Purification and Crystallization. Retinol-binding protein and transthyretin were purified from outdated human plasma as previously described (*12*). RBP was further purified by FPLC on a mono Q column eluted with a 0−500 mM NaCl gradient in 10 mM Tris (pH 8.0). TTR was further purified by affinity chromatography. Highly purified RBP was cross-linked to Pharmacia CNBr-activated Sepharose according to the manufacturers' instructions. TTR was applied to the RBP affinity resin in phosphate buffer (50 mM sodium phosphate, 50 mM NaCl, pH 7.5) and eluted with distilled water.

For the initial crystallization experiments, the complex as isolated from plasma with a 1:1 RBP:TTR stoichiometry was utilized. Substantial amounts (>35 mg) of the 1:1 complex are readily purified from ∼1.7 L of outdated plasma by modification of the protocol of Shingelton et al. (*12*). Fractions eluted from a Sephadex G-75 column which contain both TTR and RBP are further purified by anion-exchange chromatography on a Pharmacia mono Q column (10 mM Tris·HCl, pH 8.0, 0−500 mM NaCl). Free RBP elutes at ∼35% of the gradient and the complex at ∼70% of the gradient. Crystals were initially grown from hanging drop vapor diffusion room temperature experiments in which a volume of protein at 17 mg/mL was mixed with an equal volume of 1.8 M Li_2SO_4 and 40 mM Hepes (pH 7.4−8.0) and suspended above a well solution of the same components. The crystals which resulted from these trials diffracted to only 8 Å resolution. A comparison of crystal protein content with mother liquor protein content indicated that the crystal contained both RBP and TTR. In contrast, the mother liquor contained TTR but no RBP. This observation led us to conclude that the complex most likely crystallized in a 2:1 RBP:TTR stoichiometry. Furthermore, the unit cell volume could readily accommodate a 96 000 Da complex (a unit cell with 2RBP and 1TTR in the asymmetric unit would have 3.2 $Å^3$/kDa). Subsequently, dynamic light scattering experiments were performed to determine the optimal ratio of RBP to TTR necessary to ensure a complex ratio of 2:1 RBP:TTR. The apparent molecular masses of the TTR, RBP, and complex solutions at ratios of 0.5:1.0, 1:1 2:1, and 3:1 (RBP:TTR) were measured in a Protein Solutions DP801. A plot of the apparent molecular mass versus RBP:TTR ratio is hyperbolic. From this curve, it was estimated that TTR is saturated at ratios above 2:1 RBP:TTR at concentrations of ∼3 μM complex. The results of these experiments (data not shown) indicated that although virtually all RBP is bound to TTR when equimolar amounts of protein are used, a ratio as high as 3:1 RBP:TTR may be required to ensure that TTR is fully complexed. Although it is certainly preferable for the protein solution in a crystallization experiment to be monodisperse, these results indicated the necessity of adding an excess of RBP. In subsequent crystallization experiments, the complex was set up at 6 mg/mL with a ratio of 2.5−3:1 RBP:TTR. To control the ratio of RBP to TTR, and minimize the introduction of additional sources of heterogeneity into the protein preparation, the components of the complex were purified individually (as described above) and the complex was reconstituted. The stoichiometry of the complex is readily calculated from an absorbance spectrum as the amount of retinol-binding protein is deduced from the retinol absorbance at 330 nm. It was presumed that since RBP was the smaller of the two proteins, the bulk of the lattice contacts would be provided by TTR and the probability of incorporating free RBP into the lattice was minimal (*13*), and consequently excess RBP may not interfere in the crystallization of the TTR−RBP complex. This assumption turned out to be invalid. As discussed below, RBP provides all the crystal packing contacts in the crystals of the complex.

Data Collection. The crystals belong to space group $P4_12_12$ with $a = b = 140.23$ Å and $c = 124.08$ Å. For cryo data collection, the crystals were quickly swiped through a mother liquor solution which contained sufficient glycerol (3%) to prevent crystallization of the mother liquor at the temperature of data collection and then flash frozen at −150 °C in the stream of nitrogen from a Molecular Structure Corp. low-temperature system. Data were collected at beamline A1 at CHESS at a crystal to detector distance of 87.0 mM (wavelength = 0.914 Å). A total of 99 1 deg oscillation frames (22 s each) were collected. The data were processed with DENZO (*14*) and produced a data set 96.4% complete to 3.18 Å with an R_{merge} of 11.7% (a total of 331 570 reflections were measured, of which 26 640 are unique) and an I/σ ratio in the highest shell of 4.4.

Structure Solution. The structure of the RBP−TTR complex was solved by the method of molecular replacement with AMoRe (*15*) as implemented in CCP4 (*16*). In contrast to what was observed for the X-ray data from chicken RBP−human TTR crystals (*10*), a tetramer of TTR was clearly a better search model than a dimer. When tetrameric TTR generated from Protein Data Bank entry 1TLM was used as a search model, a pair of peaks related by 180° was observed (peak heights 11.7, 10.5; next peak 5.1). A translation search with rotations corresponding to these peaks and subsequent refinement of the placement produced a model with a correlation coefficient of 36.2 and *R*-factor of 51.4%. No packing problems were produced with this positioning. A $2F_o - F_c$ map calculated with TTR as positioned had uninterpretable electron density in the regions where RBP was subsequently placed. A rotation search with RBP (Protein Data Bank entry 1RBP) produced a continuum of peaks (7.4, 6.9, 6.8, 6.8, ...). However, when the rotation corresponding to the highest peak was used in a translation search with TTR positioned as above, a solution with a correlation coefficient of 45.1 and an *R*-factor of 46.5% was observed. When the 1:1 model produced by this translation search was used as a search model, a clear rotation solution (13.0, next peak 7.2) was obtained. A translation search with the 1:1 model produced a model with no packing problems with a correlation coefficient of 46.7 and an *R*-factor of 45.7%. The second RBP was placed by constructing search models of the two quaternary structures possible for the 2:1 RBP:TTR: one in which the RBP's are positioned on "opposite" dimers and one in which the two RBP's are located on the "same" TTR dimer, as described for the mixed-species complex. Because of the symmetry of TTR, both models would have equivalent TTR−RBP interfaces.

Table 1: Molecular Replacement (AMoRe) Progress

search model	rotation function correlation coef	translation and 6-d refinement CC	translation and 6-d refinement *R*-factor (%)	does the solution pack?
TTR	11.7	36.2	51.4	yes
	10.5 (related by 180°)	36.2 (related by 180°)	51.4	
	next peak 5.1			
RBP	7.4	(with TTR positioned as above)		yes
	6.9			
	6.8			
	6.8	45.1	46.5	
1 to 1	13.0	46.7	45.7	yes
	next peak 7.2, 6.0			
opposite dimer model	15.3	52.0	45.4	yes
	15.3			
	next peak 6.4			
same dimer model	11.3	44.0	47.2	no
	next peak 9.1			

Models of both quaternary structures were used as search models. Only the opposite dimer model gave a clear solution (2-fold related rotation peaks of 15.3, next peak 6.4; correlation coefficient 52.0, *R*-factor 45.4% for the translation function) and a model which packs in the unit cell. These results are summarized in Table 1.

The opposite dimer model determined with AMoRe was trimmed of the RBP amino and carboxy termini because of minor packing problems with the model as positioned. The model consisted of TTR with residues 10−123 for all four chains (A, B, C, D) and RBP amino acids 3−158 (chains E and F). Full-length TTR and RBP are 127 and 183 amino acids, respectively. This model was subjected to the simulated annealing protocol of X-PLOR (*17*) with no restraints or constraints imposed on the noncrystallographic symmetry (NCS), despite the fact that the complex has 2-fold symmetry about the 2-fold axis of TTR which runs through the central channel. The resulting model was used to calculate masks and a $2F_o - F_c$ map which was subsequently averaged in CCP4 with these masks. Forty cycles of 4-fold averaging on TTR and 2-fold averaging on RBP were performed. Model M1 was constructed into the resulting map from Protein Data Bank entries 1TLM and 1RBP. The RBP density was especially clear and, with the exception of the orientation of a few rotamers and the polypeptide chain in the TTR contact regions, conformed well to the 2.1 Å resolution structure of RBP. What was particularly reassuring about the averaged map was that the map had clear density for the retinol (Figure 1), as well as for the regions of the omitted regions of protein amino and carboxy termini.

Retinol was included in model 2, and NCS restraints were imposed in model 3 and subsequent models. TTR was restrained (both main chain and side chain atoms) as a dimer in which those parts of the dimer formed by the eight-stranded β-sheet which have regular secondary structure were defined as equivalent. The RBP's were restrained in regions of regular secondary structure (main chain and side chain atoms as well).

In all cycles of rebuilding the original TTR and RBP models retrieved from the data bank were checked for fit into the electron density. The merge-atoms option in 0 (*18*) allowed for rapid insertion of coordinates from the PDB

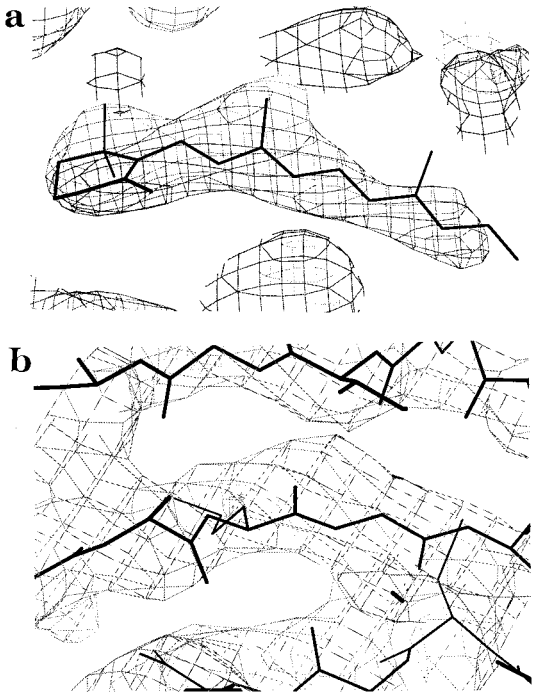

FIGURE 1: (a) Electron density for retinol in an averaged $2F_o - F_c$ map. Retinol was not included in the model. The neighboring electron density corresponds to that of the side chains which surround the ligand. (b) For comparison, a region of the electron density which corresponds to a region of the RBP model is shown.

models where indicated. Furthermore, the PDB coordinates were used without resetting the temperature factors. Instead, the *B*-factors from PDB entries 1TLM and 1RBP were adjusted by a group *B*-factor refinement in which each polypeptide chain was defined as a group. Gradually more amino and C-terminal amino acids were added to the models so that the model included A (1−124), B (10−127), C (10−123), D (10−122), E (4−183), F (4−176), and two retinol molecules. Over the course of this stage of the refinement the *R*-factor (R_{free}) dropped to 27% (42%). Regions restrained to obey the noncrystallographic symmetry had rmsd's on the order of 0.1 Å.

The low resolution of the X-ray data precluded a full refinement of the structure, but several strategies were pursued to obtain an accurate structure. For example, in all model building cycles where rebuilding was indicated, the original RBP and TTR PDB structures were checked for fit to the experimental density, and these coordinates were inserted whenever possible. However, clear differences at the RBP−TTR interface, as well as in RBP crystal packing regions, were observed, and these regions were modeled independently. Because torsion angle refinements are preferable to Cartesian refinements when determinacy is suboptimal, as is the case when only low-resolution data are available, for the later cycles of refinement we used CNS (*19*). The models produced with CNS have substantially improved geometry. In the later cycles NCS restraints were imposed on the Cα's in regions of regular secondary structure. In the final model the rms deviations for the restrained regions are on the order of 0.3 Å for both RBP and TTR. After a final *B*-factor refinement in which each amino acid was treated as a group, the final model has an *R*-factor of 27.8% and an R_{free} of 40.3%. According to PROCHECK (*20*), the parameters calculated as indicators

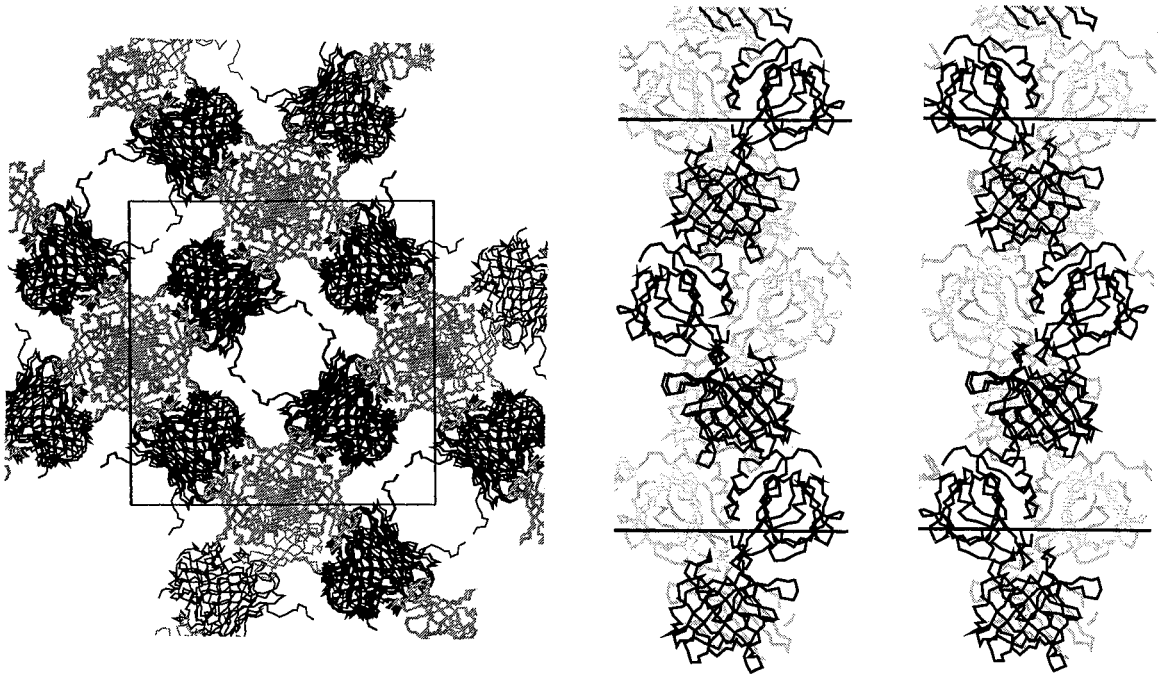

FIGURE 2: (a, left) Packing diagram for crystals of the complex. The RBP chains are in gray, and TTR is in black. (b, right) The 4-fold screw axis in space groups $P4_32_12$ and $P4_12_12$. NCS-related RBP's are in black and gray.

of good main chain and side chain stereochemistry are all inside or better than the norm for what is observed for refined structures at this resolution. A substantially lower *R*-factor can be obtained by additional refinement (<25%), but R_{free} remains intransigent. However, the fact that the structures of the individual components of the complex have been previously described and these models have been incorporated into the complex model suggests that major errors in electron density interpretation have not been made. Furthermore, addition of the carboxy-terminal amino acids to the RBP model resulted in an improvement in R_{free}. The possible sources for the problems with the *R*-factor are discussed below.

RESULTS

A packing diagram for the complex is given in Figure 2a. It is clear from this view that all protein protein contacts in the crystal are mediated by RBP−RBP interactions. The complex has a span of 120 Å, and TTR, which comprises the central 50 Å of this complex, does not participate in any packing contacts and is surrounded by very large solvent channels. As a consequence, TTR is not well restrained in the crystal lattice, an observation which is borne out by the higher average *B*-factors for TTR than RBP (62.1 vs 37.8 Å^2). The support for the crystal lattice is provided by the 4-fold screw axis composed of the 2-fold related E and F chains of RBP. The solvent content of the crystal is approximately 60%, but here at the 4-fold screw axis the RBP's pack closely together. This close approach of molecules is only possible if the loop between amino acids 161 through 169 repositions. This repositioning, which is only necessary in one of the interacting RBP monomers, can be randomly distributed throughout the crystal lattice. Therefore, a combination of localized disorder and a TTR which is only fixed indirectly in the lattice via its contacts with RBP contributes to the limited resolution of the X-ray diffraction data.

A further complication which is consistent with an intrinsic disorder in the crystal lattice is the fact that the 2-fold noncrystallographic symmetry axis of the complex is coincident with the 2-fold axis of the space group. As a result, noncrystallographic symmetry-related RBP's, as well as their crystallographic symmetry mates, spin around the 4-fold screw axis. The crystal space group might also be defined as $P4_32_12$. As described above, the structure of the complex was determined by the method of molecular replacement. The space group $P4_12_12$ was chosen over $P4_32_12$ because of the results of the translation function searches, in which the higher correlation coefficient and lower *R*-factor were obtained in the former space group. However, it became apparent in the course of the refinement that the packing of the complex in the crystal lattice could be described by either space group, but only if the noncrystallographic symmetry were strictly maintained. This observation is illustrated in Figure 2b in which the screw axes of the two space groups are depicted. The overall packing for $P4_12_12$ and $P4_32_12$ is the same, but only if both chains of RBP are identical in structure, and this is not possible because of the close packing described above. At the individual monomer level, the two diagrams clearly differ. (Attempts to refine the structure as $P4_32_12$ gave less favorable results than refinement in $P4_12_12$.) An additional source of heterogeneity is that it appears that the carboxy terminus of only one copy of RBP interacts with TTR. It is apparent from this illustration that any asymmetry in the complex could lead to heterogeneity in the lattice.

Presumably it is precisely this heterogeneity which hinders our ability to fully refine the structure. However, it can be argued that the structure we obtained is indeed accurate, despite the less than exemplary *R*-factor and R_{free}. The resolution of the data is modest, and one is dealing with a lower observation-to-parameter ratio than what is optimal. However, as mentioned above, very well defined structures for the individual components of the complex have been incorporated into the model, so presumably a poor R_{free} is

not a result of an improperly traced polypeptide chain. Second, there are two sources of heterogeneity in the crystal: (1) an asymmetric structure which may not always be incorporated into the crystal lattice in the same orientation and (2) a packing contact in the crystal lattice which necessitates a conformational change in only one copy of RBP found in the asymmetric unit. These may or may not be correlated.

The above observations suggest that the problems with R_{free} are not caused by an invalid molecular replacement solution. Indeed, the first experimental map which was calculated from model phases in which the amino- and carboxy-terminal regions of the six polypeptides, as well as the retinol in the RBP binding sites, were omitted revealed clear electron density for much of the termini and for the retinol as well (Figure 1). Furthermore, clear side chain and main chain density for the regions of RBP which differed from the uncomplexed RBP structure was evident.

DISCUSSION

Quaternary Structure of the RBP−TTR Complex. As mentioned above, well-refined structures are available for both retinol-binding protein and transthyretin. In addition, the structure of the mixed-species complex of chicken RBP and human TTR, in a stoichiometry of 2:1, has also been determined. The structure of the complex of human RBP−human TTR reveals an alternate quaternary structure and a more extensive protein−protein recognition interface, a result of the interaction of the carboxy terminus of human RBP with TTR, than what was described for the heterologous complex. Several observations suggest that the latter interaction is of physiological relevance.

The structure of the complex of RBP and TTR is shown in Figure 3. TTR is a dimer of dimers, and for the sake of discussion the polypeptide chains will be referred to as A through D. Intermonomer contacts between the monomers depicted in the upper (A and B) and lower (C and D) halves of the figure are via β-sheet contacts: each monomer contributes four β-strands to the eight-stranded β-sheet. In contrast, contacts between the upper and lower halves are much less substantial, so that the dimer assembly unit of TTR is best defined as the monomers which are joined by β-strand hydrogen bonding. As mentioned above, two molecules of RBP are complexed with TTR. The two RBP's (polypeptide chains E and F) are bound to "opposite dimers" since the bulk of the contacts are made with monomer D for RBP-E and monomer B for RBP-F. In contrast, the quaternary structure of the mixed-species complex is such that the two RBP's make the bulk of the contacts with monomers of the same TTR dimer (monomers A and B). This difference in quaternary structure could simply be a result of the fact that the symmetry of the TTR tetramer allows for the formation of equivalent interactions with RBP in two possible modes. Perhaps the two modes are available to both the mixed-species complex and the human−human complex, and crystal packing requirements have simply selected for the observed configurations. However, this may not be the case since we see an asymmetry in the relationship of the RBP's with TTR in our structure: RBP-E has more extensive interactions (the details of this interaction are described below) with TTR than molecule RBP-F. Unfortunately, the limited resolution of the X-ray data rules out the definition of a structural basis for a possible quaternary structure preference.

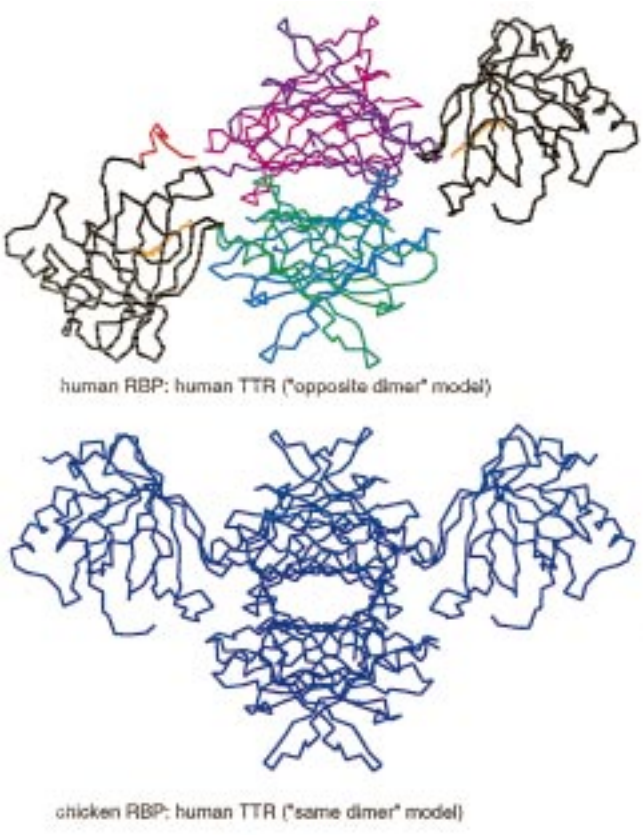

FIGURE 3: Quaternary structure of the complex of human RBP and human TTR ("opposite dimer" model) and chicken RBP and human TTR ("same dimer" model). The colors of the TTR monomers for the human−human complex correspond to those used in Figure 4 (A = magenta, B = purple, C = cyan, and D = green). The RBP molecules are in gray, and retinol is in orange. The C-terminus of human RBP is highlighted in red.

The Carboxy Terminus of RBP Is at the RBP−TTR Interface. The more intriguing structural difference between the two complex structures is the fact that an interaction with the carboxy terminus of RBP with TTR is revealed in the human−human complex. All mammalian RBP's have a carboxy-terminal extension (eight amino acids) not found in chicken RBP. In our structure we see a clear interaction of this region with TTR: the carboxy terminus of RBP-E is found nestled in the RBP−TTR interface. The terminal Leu-182−Leu-183 is burrowed in a hydrophobic patch which includes Leu(A82) from TTR and Val-E69 of RBP. Furthermore, the free carboxylate is in position to be neutralized by Arg-A21. This interaction provides as much as 40% more buried surface area when compared to the area buried in the absence of the carboxy terminus of RBP (~1400 Å).

Support for a physiological interaction of the C-terminus of RBP with TTR comes from studies on RBP clearance. As mentioned above, the formation of complex limits the loss of RBP through glomerular filtration. As early as 1971 a truncated form of RBP missing the C-terminal peptide which includes Arg-180 was shown to have a reduced affinity for TTR (*21*). More recent observations suggest an enhanced loss of truncated RBP's relative to the loss of full-length RBP. Jaconi et al. (*22*, *23*) have identified elevated levels

Table 2: Amino Acids with Accessible Surface Areas Reduced by the Formation of the Complex of TTR and RBP

TTR	Val-A20 Arg-A21	Ala-A81 Leu-A82 Gly-A83 Ile-A84	Thr-C96 Asp-C99 Ser-C100 Arg-C-103	Val-D20 Arg-D21	Lys-D76 Lys-D80 Ala-D81 Leu-D82 Gly-D83 Ile-D84 Ser-D85 Pro-D86	Tyr-D114
RBP		Leu-35 Phe-36	Leu-63 Leu-64 Asn-65 Asn-66 Trp-67 Asp-68	Lys-89 Trp-91 Gly-92 Val-93 Ser-95 Phe-96 Leu-97 Gln-98 Lys-99	Glu-179 Asn-181 Leu-182 Leu-183	

of RBP truncations in which one and two of the terminal leucines (RBP1 and RBP2, respectively) are missing in patients in whom glomerular filtration is impaired. An increase in the ratio of RBP2:RBP in these patients (relative to that observed in individuals without renal failure) suggests that RBP2 is cleared more rapidly than full-length RBP in normal circumstances. A reduced affinity of RBP2 for TTR would allow for preferential clearance of truncated forms.

Nature of the RBP−TTR Interface. The protein−protein recognition site in the RBP−TTR complex involves the positioning of the open end on the RBP β-barrel, the most likely entrance to the ligand binding cavity, at one of the 2-fold dimer axes of TTR. (A 180° rotation about this axis would superimpose the AB dimer onto the CD dimer. A second 2-fold dimer axis runs through the central thyroxine binding cavity.) The accessible surface area of 42 amino acids (Table 2, Figure 4) is reduced by complex formation, and RBP and TTR contribute 21 amino acids each to the interface. As is typical for protein−protein interaction sites, hydrophobic amino acids are at the center of the site and charged amino acids at the periphery of the site. Leu and Ile are the predominant amino acids. Half of the amino acid side chains are hydrophobic or aromatic (16 and 5, respec-

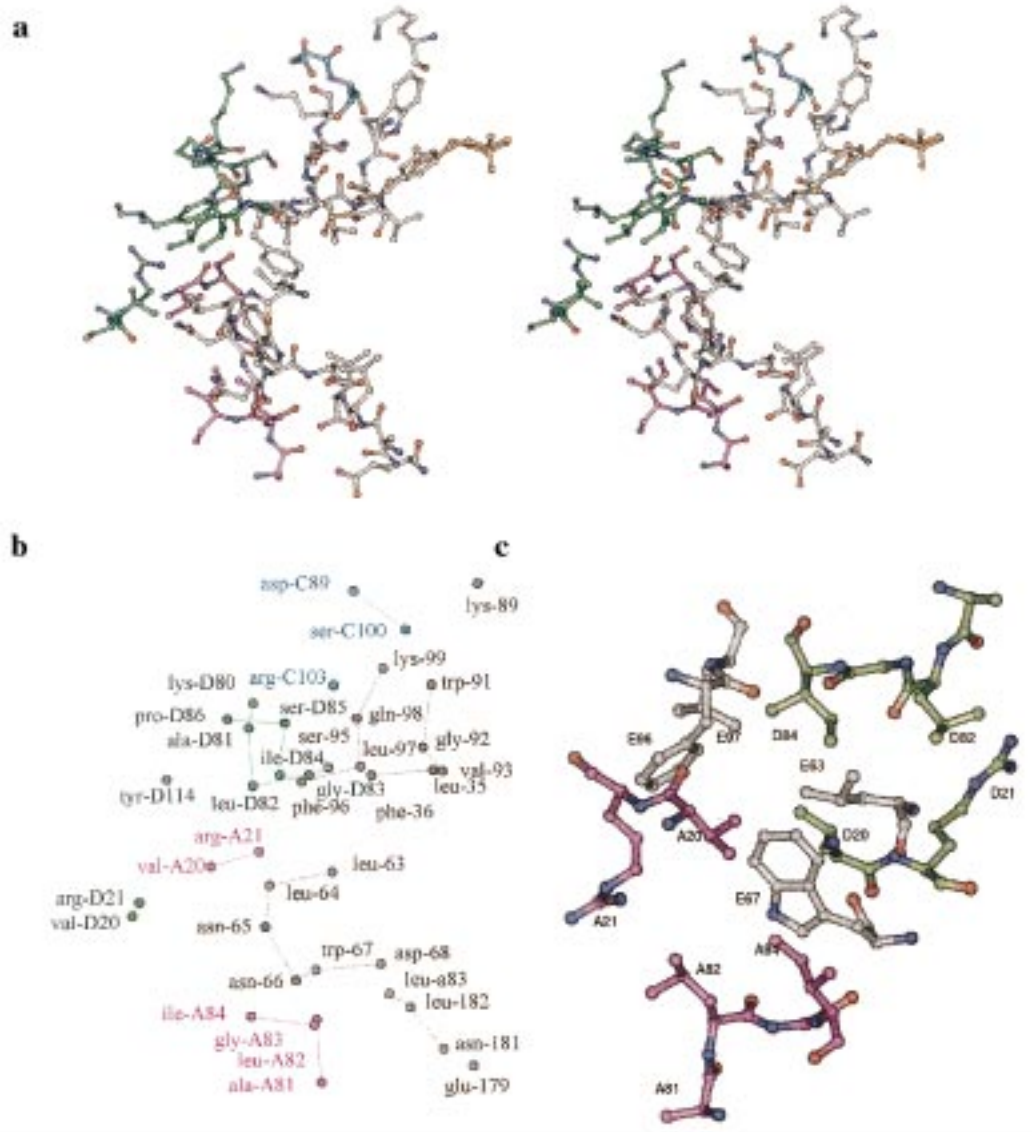

FIGURE 4: RBP−TTR interface. (a) The three polypeptide chains which make contact with RBP (E) are magenta (A), cyan (C), and green (D). Retinol is in orange, and RBP is in gray. (b) Key for (a). Only the α-carbons are displayed. (c) Diagram in which the amino acids from TTR which occur twice in the RBP binding site are illustrated.

tively). Ile-84 from TTR monomers A and D is at the core of the RBP-E interface as well as Val-20 and Ala-81 from monomers A and D. In other words, a monomeric RBP presents two different complementary surfaces to a dimeric surface. This is analogous to what has been observed for the monomeric growth hormone binding to its dimeric receptor (*24*). In both cases the monomeric protein is bivalent and presents two complementary surfaces able to interact with two copies of the same protein face on the dimer. A mutation in Ile-84 in TTR has tremendous consequences [the K_d for the RBP−TTR complex is ∼0.4 μM, whereas the affinity of I84S TTR for RBP is negligible (*25*)] because that particular amino acid occurs twice in the binding site. A diagram of this region is given in Figure 4c. Note that Trp-67, Phe-96, and Leu-63 and -97 from RBP are flanked by Val-20, Leu-82, and Ile-84 from TTR chains A and D. Clearly, substitution of Ile-84 by Ser or Asn would eliminate a significant portion of the hydrophobic core of the interaction interface.

In their description of the mixed-species complex Monaco et al. (*10*) described the basis for the observations that apo-RBP has a reduced affinity for TTR. From the illustration in Figure 4 it is clear that access to the ligand-binding cavity of RBP is further obscured by TTR. A conformational difference between apo- and holo-RBP which involves amino acids 34−37 of RBP in one of the entrance loops has been described (*26*). This loop is part of the RBP recognition surface and in apo-RBP would not be positioned for favorable interaction with TTR.

Specific protein−protein recognition can be classified in one of two basic modes: (1) a three-dimensional docking model in which two complementary three-dimensional surfaces allow for specific recognition and (2) a peptide-in-groove mode wherein a stretch of peptide from one protein fits into a groove on the three-dimensional surface of another protein. In the latter case a substantial portion of the binding surface appears to be contributed by a consecutive stretch of amino acids from the target protein and can therefore be faithfully mimicked by a peptide. Crystal structures that illustrate both modes have been described (e.g., refs *26* and *27*). As amino acids from three of the four TTR monomers and from four distinct regions of RBP form the recognition interface (Figure 4, Table 2) of the RBP−TTR complex, the structure we describe here clearly represents an example of a three-dimensional docking mode in protein−protein recognition.

ACKNOWLEDGMENT

We thank David Ong for helpful comments on the manuscript and for encouragement throughout the course of this work. X-ray data were collected at CHESS beamline A1 with the gracious help of the staff.

REFERENCES

1. Ronne, H., Ocklind, C., Wiman, K., Rask, L., Obrink, B., and Peterson, P. A. (1983) *J. Cell Biol. 96*, 907−910.
2. Soprano, D. R., and Blaner, W. S. (1994) in *The Retinoids* (Sporn, M. B., Roberts, A. B., and Goodman, D. S., Eds.) pp 257−282, Raven Press, New York.
3. Davis, J. T., and Ong, D. E. (1992) *Biol. Reprod. 47*, 528−533.
4. Ong, D. E., Davis, J. T., O'Day, W. T., and Bok, D. (1994) *Biochemistry 33*, 1835−1842.
5. Jaworowski, A., Fang, Z., Khong, T. F., and Augusteyn, R. C. (1995) *Biochim. Biophys. Acta 1245*, 121−129.
6. Kanai, M., Raz, A., and Goodman, D. (1968) *J. Clin. Invest. 47*, 2025−2044.
7. Blake, C. C. F., Geisow, M. J., Oatley, S. J., Rerát, B., and Rerát, C. (1978) *J. Mol. Biol. 121*, 339−356.
8. Cowan, S. W., Newcomer, M. E., and Jones, T. A. (1990) *Proteins: Struct., Funct., Genet. 8*, 44−61.
9. Waits, R. P., Yamada, T., Uemichi, T., and Benson, M. D. (1995) *Clin. Chem. 41*, 1288−1291.
10. Monaco, H. L., Rizzi, M., and Coda, A. (1995) *Science 268*, 1039−1041.
11. Kopelman, M., Cogan, U., Mokady, S., and Shinitzky, M. (1976) *Biochim. Biophys. Acta 439*, 449−460.
12. Shingleton, J. L., Skinner, M. K., and Ong, D. E. (1989) *Biochemistry 28*, 9641−9647.
13. Stura, E. A., and Wilson, I. A. (1992) in *Crystallization of Nucleic Acids and Proteins: A Practical Approach* (Ducruix, A., and Giege, R., Eds.) pp 99−126, Oxford University Press, Oxford, U.K.
14. Otwinoski, L. (1993) in *CCP4 Study Weekend, Data Collection and Processing* (Sawyer, L., Issacs, N., and Bailey, S., Eds.) pp 56−62, SERC Daresbury Laboratory, Warrington, U.K.
15. Navaza, J. (1994) AMoRe: an automated package for molecular replacement, *Acta Crystallogr. D50*, 157−163.
16. Collaborative Computing Project, No. 4 (1994) *Acta Crystallogr. D50*, 760−763.
17. Brunger, A. T., Kuriyan, J., and Karplus, M. (1987) *Science 235*, 458−460.
18. Jones, T. A., Cowan, S., Zou, J.-Y., and Kjelgaard, M. (1991) *Acta Crystallogr. A47*, 110−119.
19. Rice, L. M., and Brunger, A. T. (1994) *Proteins: Struct., Funct., Genet. 19*, 277−290.
20. Laskowski, R. A., MacArthur, M. W., Moss, D. S., and Thornton, J. M. (1993) PROCHECK: a program to check the stereochemical quality of protein structures, *J. Appl. Crystallogr. 26*, 283−291.
21. Rask, L., Vahlquist, A., and Peterson, P. A. (1971) *J. Biol. Chem. 21*, 6638−6646.
22. Jaconi, S., Rose, K., Hughes, G. J., Saurat, J. H., and Siegenthaler, G. (1995) *J. Lipid Res. 36*, 1247−1253.
23. Jaconi, S., Saurat, J. H., and Siegenthaler, G. (1996) *Eur. J. Endocrinol. 134*, 576−582.
24. De Vos, A. M., Ultsch, M., and Kassiakoff, A. A. (1992) *Science 255*, 306−312.
25. Berni, R., Malpeli, G., Folli, C., Murrell, J. R., Liepnieks, J. J., and Benson, M. D. (1994) *J. Biol. Chem. 269*, 23395−23398.
26. Zanotti, G., Berni, R., and Monaco, H. L. (1993) *J. Biol. Chem. 268*, 10728−10738.
27. Eck, M. J., Atwell, S. K., Shoelson, S. E., and Harrison, S. C. (1994) *Nature 368*, 764−769.

BI982291I